



# Paleoceanography and Paleoclimatology

## RESEARCH ARTICLE

10.1002/2016PA003082

### Key Points:

- Winter sea surface temperatures ( $SST_w$ ) were reconstructed in the southern Okinawa Trough over the past ~1000 years
- $SST_w$  can be used to reveal variations in the East Asian winter monsoon (EAWM) in the region
- A positive correlation is found between the EAWM and Arctic Oscillation with the reduction in Arctic sea ice cover

### Supporting Information:

- Supporting Information S1
- Data Set S1

### Correspondence to:

D. Li,  
lidongling@nbu.edu.cn

### Citation:

Li, D., Li, T., Jiang, H., Björck, S., Seidenkrantz, M.-S., Zhao, M., ... Knudsen, K. L. (2018). East Asian winter monsoon variations and their links to Arctic sea ice during the last millennium, inferred from sea surface temperatures in the Okinawa Trough. *Paleoceanography and Paleoclimatology*, 33, 61–75. <https://doi.org/10.1002/2016PA003082>

Received 28 DEC 2016

Accepted 28 NOV 2017

Published online 8 JAN 2018

## East Asian Winter Monsoon Variations and Their Links to Arctic Sea Ice During the Last Millennium, Inferred From Sea Surface Temperatures in the Okinawa Trough

Dongling Li<sup>1</sup> , Tiegang Li<sup>2,3,4</sup> , Hui Jiang<sup>5</sup> , Svante Björck<sup>6</sup> , Marit-Solveig Seidenkrantz<sup>7</sup> , Meixun Zhao<sup>8,9</sup> , Longbin Sha<sup>1,3</sup> , and Karen Luise Knudsen<sup>7</sup> 

<sup>1</sup>Department of Geography and Spatial Information Technology, Ningbo University, Ningbo, China, <sup>2</sup>Key Laboratory of Marine Sedimentology and Environmental Geology, First Institute of Oceanography, SOA, Qingdao, China, <sup>3</sup>Laboratory for Marine Geology, Qingdao National Laboratory for Marine Science and Technology, Qingdao, China, <sup>4</sup>University of Chinese Academy of Sciences, Beijing, China, <sup>5</sup>Key Laboratory of Geographic Information Science, East China Normal University, Shanghai, China, <sup>6</sup>Department of Geology, Lund University, Lund, Sweden, <sup>7</sup>Centre for Past Climate Studies and Arctic Research Centre, Department of Geoscience, Aarhus University, Aarhus C, Denmark, <sup>8</sup>Key Laboratory of Marine Chemistry Theory and Technology (Ocean University of China), Ministry of Education/Laboratory of Marine Ecology and Environmental Science, Qingdao National Laboratory for Marine Science and Technology, China, <sup>9</sup>Institute of Marine Organic Geochemistry, Ocean University of China, Qingdao, China

**Abstract** The East Asian winter monsoon (EAWM) significantly impacts living conditions in a large part of Asia, and therefore, it is important to understand its major driving mechanisms. Winter sea surface temperature ( $SST_w$ ) and circulation in the southern Okinawa Trough are today both primarily controlled by the EAWM. Here we present a new  $SST_w$  reconstruction for the last millennium based on a diatom record from sediment core MD05-2908, from the continental slope of the southern Okinawa Trough off northeastern Taiwan. Our reconstruction indicates that  $SST_w$  varied between 14.1 and 19.6°C over the past 1,000 years. Changes in  $SST_w$  in the southern Okinawa Trough correspond closely to the index of warm winters based on historical documents from the East Asian monsoon domain. This implies that our  $SST_w$  record can be used to reconstruct EAWM variability during the last millennium. Comparisons with the reconstructed winter Arctic Oscillation (AO, developed from historical snow anomaly events in Eastern Asia) and Arctic sea ice cover reveal a significant positive correlation between the EAWM and AO during the time interval from 1000–1400 Common Era (C.E.), coinciding with reduced sea ice cover. However, there is no significant correlation with increased sea ice cover during the interval from 1400 to 1700 C.E. This suggests that the reduction in Arctic sea ice may periodically have played a role in strengthening the relationship between the EAWM and the AO during the last millennium and that the current and future reduction in Arctic sea ice may have significant consequences for the EAWM.

## 1. Introduction

The Okinawa Trough, separating the East China Sea and the Pacific Ocean (Figure 1), is ideally located for paleoclimatic and paleoceanographic studies for several reasons (Li et al., 2001). First, the Okinawa Trough has a mean water depth of over 1,000 m, and therefore, it can be expected to have experienced continuous sedimentation in the late Quaternary (Peltier & Fairbanks, 2006). Second, it has extremely high sedimentation rates due to the huge input of fluvial material (Diekmann et al., 2008; Li et al., 2009), enabling high-resolution paleoclimate studies (Wei, Mii, & Huang, 2005). Third, the hydrology of the Okinawa Trough is subject to the strong influence of the East Asian Monsoon (EAM) and the Kuroshio Current, both of which play important roles in regulating heat and precipitation in densely populated East Asia (Ruan et al., 2015; Salisbury & Wimbush, 2002; Wu et al., 2012).

For these reasons, the paleoenvironment of the Okinawa Trough has attracted considerable research interest (e.g., Diekmann et al., 2008; Dou et al., 2010; Kao et al., 2008; Li et al., 2001; Sun et al., 2005; Ujiie et al., 2001; Xiang et al., 2007; Zhao, Huang, & Wei, 2005). Sea surface temperature (SST) is a key environmental parameter in oceanography and meteorology due to its important influence on exchange processes at the air-sea interface. Numerous SST records from the southern to northern Okinawa Trough have been reconstructed using

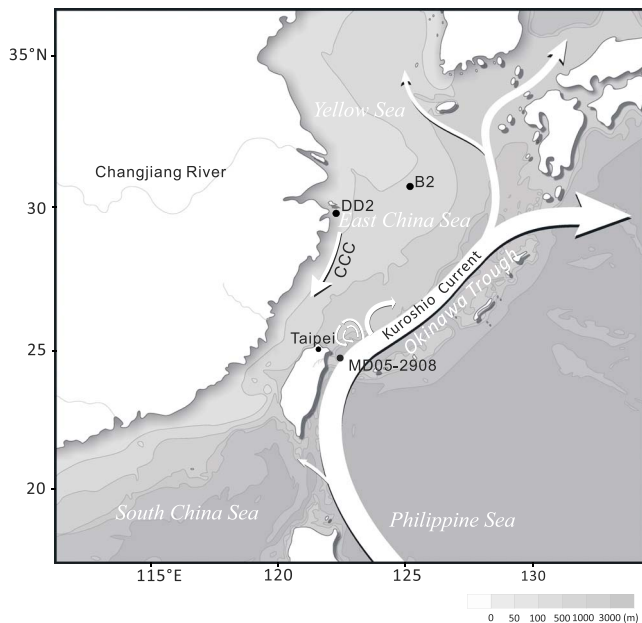


**Figure 1.** Location of sediment core MD05-2908 in the southern Okinawa Trough and the modern ocean circulation system in the study area. CCC = China Coastal Current.

various proxies (Kubota et al., 2010; Kubota, Tada, & Kimoto, 2015; Li et al., 2001; Li, Jian, & Wang, 1997; Lin et al., 2006; Ruan et al., 2015; Wu et al., 2012; Xiang et al., 2003, 2007; Yu et al., 2009). Chang et al. (2008) estimated the millennial-scale SST variability of the past 40 kyr in the central Okinawa Trough based on planktonic foraminiferal fauna assemblages, and by analyzing long-chain alkenones in Ocean Drilling Program core 1202B. In addition, Zhao et al. (2005) and Lin et al. (2006) reconstructed the paleo-SST in the southern Okinawa Trough based on alkenones and Mg/Ca ratios of planktonic foraminifera, respectively. Subsequently, Wu et al. (2012) and Ruan et al. (2015) used the same core to estimate SST variability based on TEX<sub>86</sub> and long-chain alkenone records, respectively. Most of the current proxy-based SST reconstructions show variations in mean annual SST with a decadal to centennial time resolution. However, winter SST ( $SST_w$ ) reconstructions are scarce, except for a planktonic foraminiferal-based  $SST_w$  and a TEX<sub>86</sub>-based  $SST_w$  reconstruction in the southern and northern Okinawa Trough, respectively (Jian et al., 2000; Nakanishi et al., 2012). Consequently, new high-resolution and independent records based on new types of environmental proxy are needed to quantify  $SST_w$  changes in the region.

The East Asian monsoon (EAM), consisting of the East Asian summer monsoon (EASM) and the East Asian winter monsoon (EAWM), is a major component of the climate of East Asia. It exerts a direct impact

on temperature and precipitation in the region, and consequently influences the occurrence of extreme climate events and disasters, such as floods and severe cold winters (Wang et al., 2005). Past variability of the EASM during the Holocene has been investigated in many  $\delta^{18}O$  isotope studies of Chinese cave stalagmites (e.g., Dykoski et al., 2005; Hu et al., 2008; Li et al., 2015; Wang et al., 2005; Zhang et al., 2008; Zhao et al., 2015). On the other hand, compared with the EASM, records of the EAWM are sparse owing to the limited number of suitable archives and proxies (Sagawa et al., 2014). Grain size of sediments and foraminiferal  $\delta^{18}O$  records from marine sediments and elemental ratios in Chinese loess deposits are commonly used proxies for reconstructing of the Holocene EAWM strength (Hu et al., 2012; Liu et al., 2010; Sagawa et al., 2014; Xiang et al., 2006; Xiao et al., 2006; Yang et al., 2015; Zheng et al., 2014; Zhou et al., 2014). However, the trends of EAWM intensity reconstructed for the last millennium from different sediment cores tend to be inconsistent and even contradictory (Tian, Huang, & Pak, 2010; Wu et al., 2012, 2014; Xiang et al., 2006; Xiao et al., 2005; Zhou et al., 2014). The discrepancies between different records indicate that more high-resolution reconstructions, based on other types of proxy, are needed to reliably characterize variations in EAWM strength. The EAWM is considered to have a strong influence on changes in  $SST_w$ , and the reconstruction of  $SST_w$  is therefore an excellent tool for reconstructing the EAWM (Tian et al., 2010; Wu et al., 2012, 2014). The factors that may influence the EAWM include the El Niño–Southern Oscillation (He & Wang, 2013a; Lau & Nath, 2000; Wang & He, 2012; Webster & Yang, 1992; Zhang, Sumi, & Kimoto, 1996), the Arctic Oscillation (AO) (Gong, Wang, & Zhu, 2001; He & Wang, 2013b; Wu & Wang, 2002), the Antarctic Oscillation (Fan & Wang, 2004, 2006), conditions on the Tibetan Plateau and Eurasian snow cover (Walland & Simmonds, 1996; Watanabe & Nitta, 1999), and Arctic sea ice (Li & Wang, 2013a, 2013b; Liu et al., 2012). Based on data reanalysis from the National Centers for Environmental Prediction (NCEP) and National Center for Atmospheric Research and the Hadley Centre Ice Sea Surface Temperature data set (HadISST) (Rayner et al., 2003), Li and Wang (2014) found that the reduction of autumn Arctic sea ice cover in the region of 67–85°N, 30–135°E resulted in a strengthening of the AO-EAWM relationship during the time interval of 1983–2012 Common Era (C.E.). In contrast, there was an insignificant correlation between the AO and EAWM during the interval 1950–1970 C.E. However, it is unclear if this intermittent relationship between the AO and EAWM is typical.

Diatoms are one of the most sensitive and robust indicators in paleoceanographic and paleoclimatic studies, and are widely used as a proxy for SST, such as diatom temperature ( $Td'$ ) values (Kanaya & Koizumi, 1966; Koizumi et al., 2006) and SST reconstructions based on diatom-transfer functions (Berner et al., 2008; Birks

& Koç, 2002; Jiang et al., 2015; Justwan & Koç, 2008; Miettinen et al., 2011). They are also used as a proxy for past sea ice variability (e.g., sea ice concentration and IP25) in both the Northern and Southern Hemispheres (e.g. Belt et al., 2007; Crosta, Pichon, & Burckle, 1998; de Vernal et al., 2013; Krawczyk et al., 2017, 2010; Müller et al., 2009; Sha et al., 2014, 2017, 2016). A previous study showed that changes in surface diatom assemblages in the western Pacific marginal seas are due to variations in  $SST_w$  and summer sea surface salinity (SSS), and thus, they are the two most important environmental factors controlling the regional diatom distribution (Huang et al., 2009). Consequently, down-core diatom data can be used to reconstruct past  $SST_w$  in the region. Li et al. (2012) presented diatom assemblage data for marine sediment core MD05-2908 from the Okinawa Trough. Here we use the record above to obtain a new high-resolution (11 year) reconstruction of  $SST_w$ , making it possible to carry out a more direct comparison with other climate data. The objectives of our study are twofold: first, we quantitatively reconstruct  $SST_w$  during the last millennium in the southern Okinawa Trough, and second, we examine variations in the EAWM inferred by changes in  $SST_w$  and test the possible impact of Arctic sea ice on the relationship between the EAWM and AO during the last millennium.

## 2. Atmospheric and Oceanographic Setting

The Okinawa Trough, a curved back-arc basin in the southeastern part of the East China Sea (Figure 1), lies between 24–30°N and 122–130°E. It is about 1200 km long and 100–230 km wide. The mean water depth is ~500 m in the north and over 1000 m in the central and southern parts. Circulation in the Okinawa Trough is modulated by the EAM (Lee & Chao, 2003).

The EAM is a consequence of the thermal contrast between the Asian landmass and the tropical Pacific (Wang et al., 2009). A low-pressure cell above the central Eurasian continent during summer is associated with southeasterly winds that carry warm and moist air masses from the Pacific Ocean toward Taiwan and mainland China. During the winter season (when the EAWM is strong), reversed pressure gradients with prevailing northwesterly winds carry cool and dry air masses from the Eurasian continent toward the Pacific Ocean.

The EAM not only controls the atmospheric circulation but also strongly impacts ocean circulation. Under the intense northeastern winter monsoon, a southward coastal jet develops mainly to the south of the Changjiang River (Figure 1), extending toward the Taiwan Strait. The resulting strong winds drive the formation of the so-called China Coastal Current (CCC; Figure 1), which is further enhanced by the stratification provided by the Changjiang runoff. Modeling results indicate that the strength of the CCC peaks in December and diminishes with the winter monsoon in March (Lee & Chao, 2003).

The Kuroshio Current is a western boundary current in the North Pacific Ocean, with a depth of up to 1 km and a width of 150–200 km. It originates from the western Pacific warm pool, flows along the east coast of Taiwan, and then along the continental slope in the East China Sea, eventually turning eastward south of Japan (Salisbury & Wimbush, 2002).

## 3. Material and Methods

### 3.1. Sediment Core

Piston core MD05-2908 (24°48.04'N, 122°29.35'E; Figure 1) is 34.16 m in length and was obtained from the continental slope of the southern Okinawa Trough off northeastern Taiwan, in a water depth of 1276 m, during the *R/V Marion Dufresne IMAGES XII* cruise in 2005. Samples were analyzed every 8 cm for their diatom content, yielding a mean sample resolution of ~11 years for the entire ~1,000 year interval studied. The samples were prepared following the method described by Håkansson (1984). All samples were treated with 10% HCl to remove calcareous material followed by 30% H<sub>2</sub>O<sub>2</sub> (1–2 h in a water bath at 60 °C) to remove organic material. Samples with a high proportion of clay were washed repeatedly by suspending and dispersing the material in distilled water in a 100 mL beaker. The supernatant was decanted off after a minimum of 3–5 h. An aliquot of the shaken suspension was placed on a cover slip and mixed with a pipette to distribute the diatoms evenly. After the material had completely dried, the cover slips were transferred onto permanently labeled slides, mounted with Naphrax (dn = 1.73) and heated to 250°C. A Leica microscope with phase contrast at a magnification of ×1000 was used for diatom identification and counting. The relative abundance,

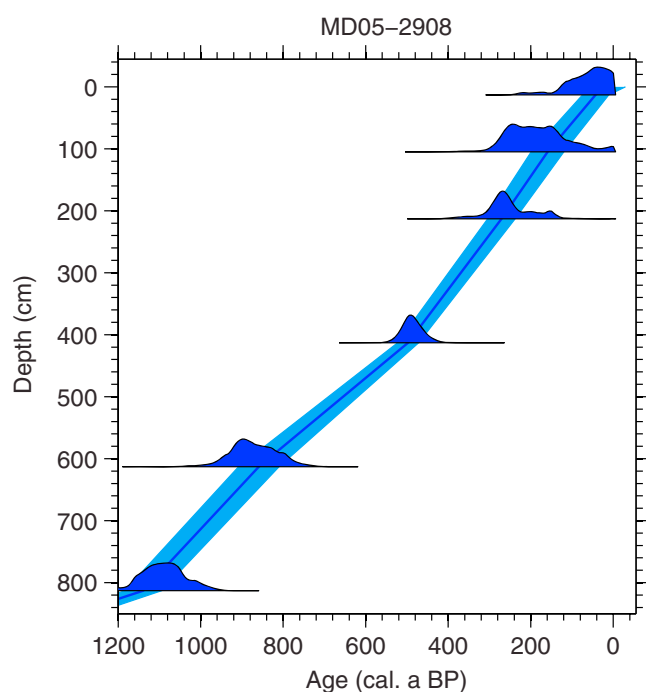


**Figure 2.** Age model based on six calibrated radiocarbon ages from the upper part of core MD05-2908 (see Table S1 in the supporting information; Li et al., 2012).

environmental variables, including summer and winter SST and SSS (Huang et al., 2009). Canonical correspondence analysis, a direct gradient analysis, was used to study the variations in the surface sediment diatoms that can be explained by a specific set of environmental variables (in this case, summer and winter SST and SSS; see Figure S1 in the supporting information).

The variance inflation factor (VIF) is used to evaluate if each variable has a unique influence on the modern diatom distribution (ter Braak & Smilauer, 2002). The VIF tests the significance of multicollinearity in the regression analysis, determining how much of the variance of the regression coefficient is increased because of collinearity. The VIF values of all four variables are less than 20, suggesting that multicollinearity among these four variables is low.

In addition, forward selection of the environmental variables and associated Monte Carlo permutation tests of the statistical significance of each variable were used to test if all four variables were individually significant ( $p = 0.001$ , 999 permutations). Marginal effects indicated the variability of each explanatory variable without considering other environmental factors. Conditional effects denoted the influence of each variable after removing the confounding effect of one or more of the other covariables. Among them,  $SST_w$  and summer SSS captured most of the canonical variance (winter SST, 0.36; summer SSS, 0.34; summer SST, 0.13; and winter SSS, 0.09), suggesting that  $SST_w$  is one of the two most important environmental factors controlling the distribution of diatoms in the surface sediments (Huang et al., 2009). Therefore, it can potentially be used for  $SST_w$  reconstruction.

A revised modern calibration data set from the western Pacific marginal seas (Table S2 in the supporting information) was used to generate a diatom-based transfer function for quantitative reconstruction of  $SST_w$ . The computer program C2, a software package widely used for (paleo) ecological data analysis and illustration (Juggins, 2003), was used for the  $SST_w$  reconstruction. Seven numerical reconstruction methods were tested to determine the optimal diatom-based  $SST_w$  transfer function (Table 1). The weighted averaging partial least squares (WA-PLS) method with three components resulted in a low root-mean-squared error of prediction ( $RMSEP_{(Jack)}$ ) (1.78), a low maximum bias (1.83), a high squared correlation ( $R^2_{(Jack)}$ ) (0.94), and the smallest number of “useful” components for reconstructing  $SST_w$  (Table 1). Furthermore, plots of jack-knife inferred  $SST_w$  against observed  $SST_w$  show a good linear correlation (Figure 3a) and the residuals are

calculated as a percentage of the total diatom assemblage, was based on counts of at least 300 diatom valves. *Chaetoceros* resting spores were excluded from the counts due to their high abundance, which would otherwise mask the signal of the remaining diatoms. Moreover, it is difficult to identify *Chaetoceros* resting spores below genus level in fossil material (Jensen et al., 2004; Justwan & Koç, 2008; Koç & Schrader, 1990; Miettinen et al., 2011; Miller et al., 2011). Consequently, they are also excluded from the modern data set used for constructing the transfer function.

### 3.2. Chronology

Six accelerator mass spectrometry (AMS)  $^{14}C$  age determinations were carried out on the planktonic foraminiferal species *Globigerinoides ruber* (white) and *G. sacculifer* (Table S1 in the supporting information) at the AMS  $^{14}C$  Dating Centre at Woods Hole Oceanographic Institution, Massachusetts, USA. The  $^{14}C$  ages were calibrated using the OxCal v. 4.13.9 program (Ramsey, 2008) with the marine calibration curve Marine09 (Reimer et al., 2009) and using the local marine reservoir age,  $\Delta R = 35 \pm 25$  years (Hideshima et al., 2001). An age model (Figure 2) was constructed using the depositional model option in OxCal with a  $k$  value of 5, yielding  $A_{model} = 85.2\%$  (Li et al., 2009).

### 3.3. Modern Data Set and Diatom-Based Transfer Function

A modern calibration data set is available from the western Pacific marginal seas, consisting of diatom data from surface sediments and four

**Table 1**  
Results of Method Testing for the Transfer Function

		Max_Bias	$R^2_{(Jack)}$	RMSEP <sub>(Jack)</sub>
WA	Inverse	4.16	0.85	2.94
WA <sub>(tol)</sub>	Inverse	3.40	0.90	2.45
WA	Classical	4.52	0.85	3.04
WA <sub>(tol)</sub>	Classical	2.58	0.90	2.48
PLS	1 component	10.55	0.35	6.11
PLS	2 components	10.29	0.54	5.14
PLS	3 components	8.16	0.66	4.44
PLS	4 components	6.01	0.82	3.18
PLS	5 components	4.81	0.86	2.86
WA-PLS	1 component	4.18	0.85	2.95
WA-PLS	2 components	2.82	0.91	2.23
WA-PLS	3 components	1.83	0.94	1.78
WA-PLS	4 components	1.01	0.95	1.66
WA-PLS	5 components	0.67	0.95	1.70
MAT	1 analogue	7.8	0.84	3.08
MAT	2 analogues	8.4	0.88	2.64
MAT	3 analogues	7.5	0.89	2.49
MAT	4 analogues	7.03	0.89	2.50
MAT	5 analogues	7.37	0.87	2.71

Note. Root-mean-squared errors (RMSE), root-mean-squared error of prediction based on leave-one out Jack-knifing (RMSEP<sub>(Jack)</sub>), Max\_Bias and  $R^2$  for the reconstructed SST<sub>W</sub> (°C) in six reconstruction procedures. WA = weighted averaging, WA<sub>(tol)</sub> = weighted averaging with tolerance down-weighting, (PLS) = partial least squares and (WA-PLS) = weighted averaging partial least squares, and MAT = modern analogue technique. Both inverse and classical deshrinking regression were used in WA and WA<sub>(tol)</sub> reconstruction procedures. The test shows that WA-PLS with three components is the most reliable (values in bold).

randomly scattered (Figure 3b). The WA-PLS with three components was therefore used for reconstructing SST<sub>W</sub> variability in the southern Okinawa Trough.

### 3.4. Time-Series Analysis

The power spectrum of the reconstructed SST<sub>W</sub> record was calculated using the Lomb-Scargle Fourier transform (Lomb, 1976; Scargle, 1982). The computations were made using the publicly available software program REDFIT (Schulz & Mudelsee, 2002), which also computes red-noise (AR1) false-alarm levels through which the dominant periodicities can be identified.

Running correlation coefficients of the reconstructed SST<sub>W</sub> and winter AO were calculated for data in 250 year sliding windows, and a random phase test was used to assess the autocorrelations present in the time series (Ebisuzaki, 1997).

## 4. Results and Discussion

### 4.1. Test of the Diatom-Based SST<sub>W</sub> Reconstruction

The reconstructed SST<sub>W</sub> of the southern Okinawa Trough varies between 14.1 and 19.6°C (with a mean value around 16.9°C) and exhibits clear decadal to centennial warm/cold variations during the last millennium (Figure 4a and Table S3 in the supporting information). To evaluate the reliability of the diatom-based SST<sub>W</sub> reconstruction as a measure of paleoceanographic changes in the southern Okinawa Trough, we compared the SST<sub>W</sub> value from the top sample of the studied core with observed data. The youngest part of core MD05-2908 has an age of 1929 C.E. based on the age model (Table S1) and the reconstructed SST<sub>W</sub> value (~15.47°C) corresponds to the observed February SST (~16.6°C) obtained from the HadISST 1.1 data set provided by the Hadley Centre for Climate Prediction and Research (2007), which is well within the reconstructed error. We also compared our reconstructed SST<sub>W</sub> record with a record of the frequency of cold winters in Guangdong and Guangxi provinces, South China, over the past 500 years with almost the same time resolution (10 years) (Zhang, 1980; Figure 5). These data are based on historical records from documents such as local gazettes. A similar pattern was observed between changes in reconstructed SST<sub>W</sub> in the southern Okinawa Trough and time series of warm and cold winters in South China, except for two short intervals of 1575–1600 and 1850–1900 C.E. This implies that our diatom-based SST<sub>W</sub>

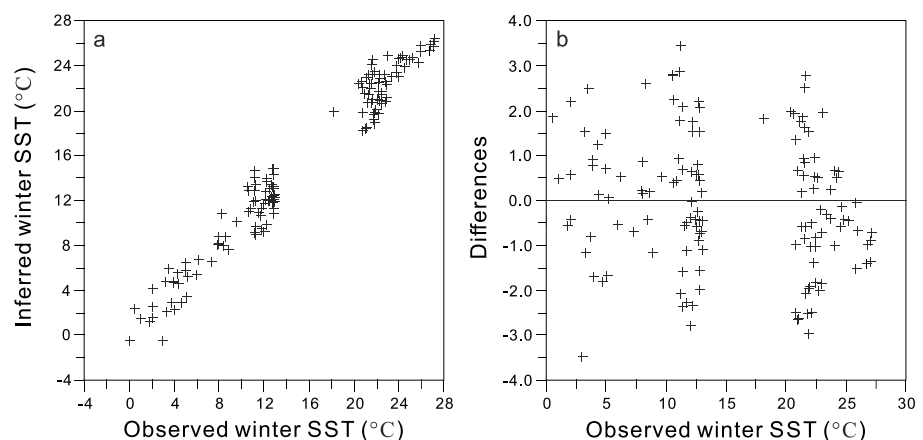


**Figure 3.** Plots of (a) jack-knife inferred SST<sub>W</sub> using WA-PLS (three components) versus observed SST<sub>W</sub> (°C) and (b) of the differences between jack-knife inferred and observed SST<sub>W</sub> (°C).

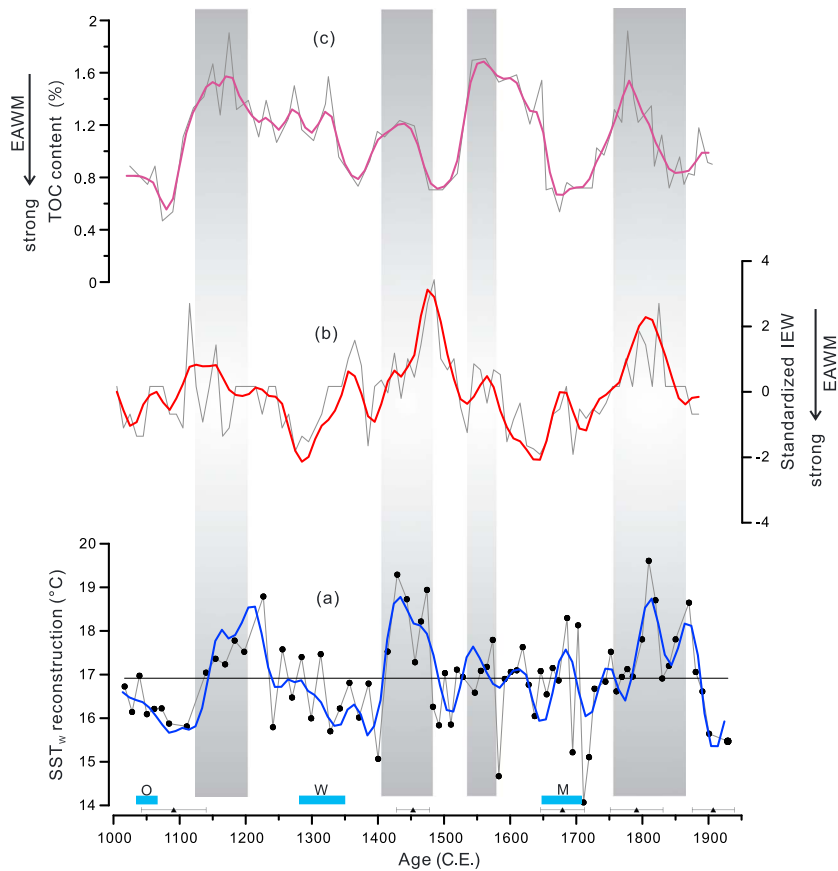


**Figure 4.** Plots with (a) reconstructed  $SST_W$  ( $^{\circ}C$ ) based on diatom data from sediment core MD05-2908 versus age (C.E.-scale) in the southern Okinawa Trough, compared with (b) the standardized index of extreme warm winter (IEW) anomalies in the Korean Peninsula (Chu et al., 2012) and (c) a TOC record from northwestern China, used as a proxy for the EAWM (Liu et al., 2009). The gray areas correspond to weak EAWM events and the blue bars to solar events (O = Oort Minimum, W = Wolf Minimum, M = Maunder Minimum). All records are low-pass filtered with a 50 year cutoff. The solid triangles on the horizontal axes show five of the six age-control points/ $^{14}C$  dates (Table S1, see also Figure 5 and Figure 7).

record is generally reliable for reconstructing paleoceanographic changes in the southern Okinawa Trough during the last millennium.

**4.2. Reconstruction of  $SST_W$**

Our  $SST_W$  record for the past 1,000 years (Figure 4a) exhibits three significantly warm intervals, with relatively high  $SST_W$ : 1130–1250, 1400–1480, and 1750–1870 C.E. They were interrupted by two cold intervals, 1300–1400 and 1500–1750 C.E. A steady increase in  $SST_W$  occurred during the interval 1100–1250 C.E., with a particularly high SST between 1150 and 1250 C.E. This indicates that the southern Okinawa Trough experienced a high frequency of warm winters at the culmination of the “Medieval Warm Period” (MWP, 950–1250 C.E).

The  $SST_W$  were generally below the mean value during the intervals 1300–1400 and 1500–1750 C.E., with three relatively distinct minima in  $SST_W$  at 1510, 1650, and 1710 C.E., suggesting significantly cold conditions in the southern Okinawa Trough. This later colder part, 1510–1770 C.E., corresponds in time to a large part of the “Little Ice Age” (LIA) dated to 1300–1850 C.E. (Keigwin, 1996; Nyberg et al., 2002).

The relatively cool climate of the LIA period was thus interrupted by the two warm intervals of 1400–1480 C.E. and 1750–1870 C.E. in our region

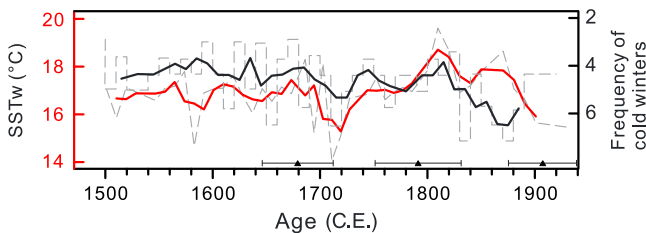


**Figure 5.** Diatom-based reconstructed  $SST_W$  (3-point running mean = red) for the interval 1500–1920 C.E. compared with the frequency of cold winters per decade in Guangdong and Guangxi, South China (3-point running mean = black), over the past 500 years. The dashed lines show the original data.

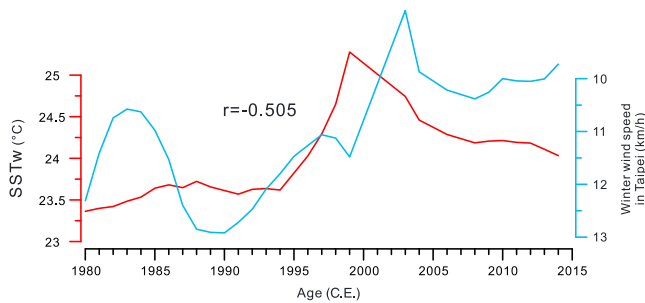


**Figure 6.** Correlation coefficient between  $SST_W$  (red) with winter wind speed in Taipei (blue), representing the East Asian winter monsoon strength in the study area for the interval 1980–2015 C.E. (3-point running means). The source of the SST data is the ICOADS data provided by the NOAA/OAR/ESRL PSD, Boulder, Colorado, USA, from their web site at <http://www.esrl.noaa.gov/psd/>. The wind speed data (December–January–February) were obtained from the observation station in Taipei and the meteorological data network <http://en.tutiempo.net/climate/>. Both the winter SST and wind speed data are average values for December, January, and February.

in Taipei ( $25^{\circ}1.8'N$ ,  $121^{\circ}31.8'E$ ) (<http://en.tutiempo.net/climate/>), very close to the study area. The results reveal a negative correlation between  $SST_W$  and winter monsoon strength in the southern Okinawa Trough ( $r = -0.505$ , at the 99% confidence level; Figure 6). When the EAWM is strong (weak), strong (weak) cold and dry northerly winds from the interior of the Asian continent blow across the East China Sea, causing more (less) intensive convection of ocean water. Consequently, large (small) amounts of heat are released to the atmosphere, causing a large (small) decrease in SST (Xie et al., 2002). Therefore, we used the variation of winter SST to infer changes in the EAWM during the last millennium: the lower the winter SST, the stronger EAWM (higher wind speed of DJF).

The relatively low and decreasing  $SST_W$  (Figure 4a) suggests an interval of intense EAWM activity between 1000 and 1100 C.E., coincident with the Oort Minimum centered around 1050 C.E. (Bard et al., 2000). Chu et al. (2012) developed an index of extreme warm winters (IEW; Figure 4b) based on the official historical documents (including History of the Three Kingdoms, Annals of Goryeo, and the Annals of the Joseon Dynasty) for the Korean Peninsula, where climate is also strongly influenced by the East Asian monsoon.  $IEW = (W_1 \times A_1 + W_2 \times A_2 + 1) / (\text{total events/per decade} + 2)$ , where  $W_1$  and  $W_2$  reflect the extremeness of winter warm events, totaled per decade. When the description “no ice in wintertime” was given in the historical document,  $W_1 = 2$ , and when the description “winter warm as spring” was given,  $W_2 = 1$ .  $A_1$  and  $A_2$  are the number of years with extreme events per decade. Total events include all extreme events, in both summer and winter, per decade (Chu et al., 2012). Among these historical documents, the Annals of the Joseon Dynasty (1392–1910 C.E.), with more than 1,800 volumes, was an especially valuable documentary source that provided daily climatic information. For example, the IEW record shows that no extreme warm winter occurred during the interval 1000–1100 C.E. (Figure 4b). In addition, Li et al. (2015) studied the  $\delta^{18}O$ ,  $\delta^{13}C$ , and XRF scanned elemental profiles of Stalagmite DGS-1 from Jianfei Cave in Dagangshan Mountain, South Taiwan, to reveal interannual variations in climate and environmental conditions. The heavier  $\delta^{18}O$  and  $\delta^{13}C$  values, as well as the low Fe content, reflect dry and cold climatic conditions with poor vegetation growth around 1050 C.E. in South Taiwan (Li et al., 2015). These cold events can generally be correlated with low diatom-based  $SST_W$  reflecting relatively strong EAWM.

Total organic carbon (TOC) is often used as a productivity proxy (Bickert & Wefer, 1999; Versteegh & Zonneveld, 2002). Liu et al. (2009) used low TOC concentrations in the sediments of Kusai Lake, northwestern China, to infer strong EAWM activity. This was based on the observation that when the winter monsoon intensifies, low precipitation and cold temperatures led to low aquatic primary productivity. A distinctly low sedimentary TOC content in Kusai Lake suggests an intensified EAWM during the interval 1000–1100 C.E. (Figure 4c) (Liu et al., 2009). In addition, grain-size data from core DD2, from the inner shelf of the East China Sea, also recorded a cold event around 1050 C.E., which might result from strong EAWM (Xiao et al., 2005). Moreover, the oxygen isotope record from the GISP2 Greenland ice core reveals a significant cooling

(Figure 4a). This suggests that the southern Okinawa Trough experienced periods with a relatively high frequency of warm winters during parts of the LIA. This is not a local but a regional phenomenon: a 500 year record of freezing dates from Lake Suwa, Japan, based on documentary evidence, indicates that warm winters were common during the LIA (Arakawa, 1954; Magnuson et al., 2000).

#### 4.3. Climatic and Oceanographic Changes During the Last Millennium: Regional and Global Correlations

The southern Okinawa Trough is in the typical East Asian monsoon region, and thus, changes in  $SST_W$  may be primarily caused by fluctuations in the intensity of the EAWM. We analyzed the instrumental data from 1980 to 2014 C.E. for the study area to examine a possible winter monsoon–temperature connection. According to Yan, Soon, and Wang (2015), the average wind speed during December, January, and February (DJF) can be used as a relative measure of EAWM strength. Therefore, we calculated the correlation coefficient between the reconstructed  $SST_W$  in the study area and the average DJF wind speed (Figure 6), which was obtained from the observation weather station

at around 1050 C.E., which indicates that the cooling event was of global scale (Stuiver & Grootes, 2000). This is in agreement with our observations of relatively low SST<sub>w</sub> in the southern Okinawa Trough during the same periods.

Subsequently, the significantly increasing SST<sub>w</sub> between 1100 and 1250 C.E., implying a weakened EAWM, corresponds well with the MWP. During the same interval, the diatom assemblages of core MD05-2908 also show an increase in the abundance of tropical species (see Figure S2 in the supporting information), consisting primarily of *Azpeitia nodulifera*, *Rhizosolenia bergonii*, and *Alveus marina*, which were used to represent increased warm water influence in the South China Sea (Jiang et al., 2004) and East China Sea (Li et al., 2012). An increased incidence of extreme warm winters in the IEW record (Figure 4b), e.g., “warm winter for a long interval in 1149 C.E.” and “no ice in December, warm as spring in 1156 C.E.,” also recorded such a weakening of the EAWM (Chu et al., 2012).

From 1250 C.E. and onward, fluctuations in EAWM strength, as revealed in our SST<sub>w</sub> record, became more frequent. Two intervals of strong EAWM from 1250–1400 C.E. and from 1500–1750 C.E. are indicated by relatively low SST<sub>w</sub> in the southern Okinawa Trough. These two intervals correlate well with two different sunspot minima, i.e., the Wolf Minimum and the Maunder Minimum (1250–1400 and 1500–1700 C.E., respectively) (Bard et al., 2000; Stuiver & Quay, 1980). The strengthened EAWM inferred by decreasing SST<sub>w</sub> at around the late thirteenth century could be linked to the large El Chichon 1259 C.E. volcanic eruption (D’Arrigo et al., 2001; Stothers, 2000). The  $\delta^{18}\text{O}$  and  $\delta^{13}\text{C}$  records, as well as the low Fe content of Stalagmite DGS-1, also suggest cold and dry conditions around 1360 C.E. (Li et al., 2015). Furthermore, a cold spell around 1300 C.E. has also been identified in proxy data from Mongolia and northern Siberia (D’Arrigo et al., 2001; Hantemirov & Shiyatov, 2002; Naurzbaev et al., 2002). Distinctly low values of the IEW and SST<sub>w</sub> also suggest an intensified EAWM during the intervals 1250–1400 and 1500–1750 C.E. (Figure 4b) (Chu et al., 2012). Relatively low sedimentary TOC contents during 1325–1390 and 1650–1750 C.E. in northwestern China also indicate an intensified EAWM (Liu et al., 2009). Environmentally sensitive grain-size components from core B2, located in an area of mud deposition southwest of Cheju Island, in the East China Sea (Figure 1), also recorded three distinct cold events, at 1350, 1590, and 1700 C.E. (Xiang et al., 2006). In addition, grain-size data from core DD2, from the East China Sea, suggest two episodes of intensified EAWM in 1510 and 1670 C.E. (Xiao et al., 2005).

The EAWM weakened during the intervals 1400–1500 and 1750–1870 C.E., as inferred by relatively high SST<sub>w</sub> in the southern Okinawa Trough (Figure 4a). The abundance of tropical species also increased during 1400–1500 and 1790–1890 C.E., suggested by the diatom assemblages of core MD05-2908 (see Figure S2 in the supporting information) (Li et al., 2012). From historical documents we note 38 years with extremely warm winters within a 100 year interval (1400–1500 C.E), described as “a winter as warm as spring in 1401, 1442, and 1479 C.E.,” “no ice in December of 1402, 1425, and 1432 C.E.,” and “pray God for cold in 1475, 1486, and 1499 C.E.” (Chu et al., 2012). Warm winters were also recorded in the interval 1750–1870 C.E.; e.g., “no ice in winter, pray God for cold in 1769 C.E.,” “a winter as warm as summer in 1776 C.E.” and “no ice in the river, as warm as spring in 1827” (Chu et al., 2012).

#### 4.4. Possible Mechanisms Controlling EAWM Variability During the Last Millennium

The variability of the EAWM depends largely on the behavior of the Siberian High (Gong & Ho, 2002) and the Arctic Oscillation (AO) (Gong et al., 2001; Li & Bates, 2007). According to Gong et al. (2001), the AO influences the EAWM via its impact on the Siberian High. When the AO is in a negative phase and the Siberian High is strong, the low temperatures at high northern latitudes result in a strong EAWM (D’Arrigo et al., 2005; Wu & Wang, 2002). Li, Wang, and Gao (2014) used NCEP reanalysis and 40 year Re-Analysis (ERA-40) data from the European Centre for Medium-Range Weather Forecasts to document the strengthened relationship between the EAWM and winter AO on an interannual timescale with a comparison of the time intervals 1950–1970 and 1983–2012 C.E. The results show that a reduction of Arctic sea ice cover was responsible for the strengthened EAWM-AO relationship during the interval 1983–2012 C.E., caused by the upstream extension of the East Asian jet stream (Li et al., 2014).

Chu et al. (2008) developed the Index of Abnormal Snow:  $\text{IAS} = (\text{NSE} + 1)/(\text{NSE} + \text{PSE} + 2)$  based on historical official documents (the 24 dynastic histories) in China and Korea (Figure 7b, [www.ncdc.noaa.gov/paleo/recons.html](http://www.ncdc.noaa.gov/paleo/recons.html)). NSE is the number of years with negative snow events (defined from direct descriptions: “no

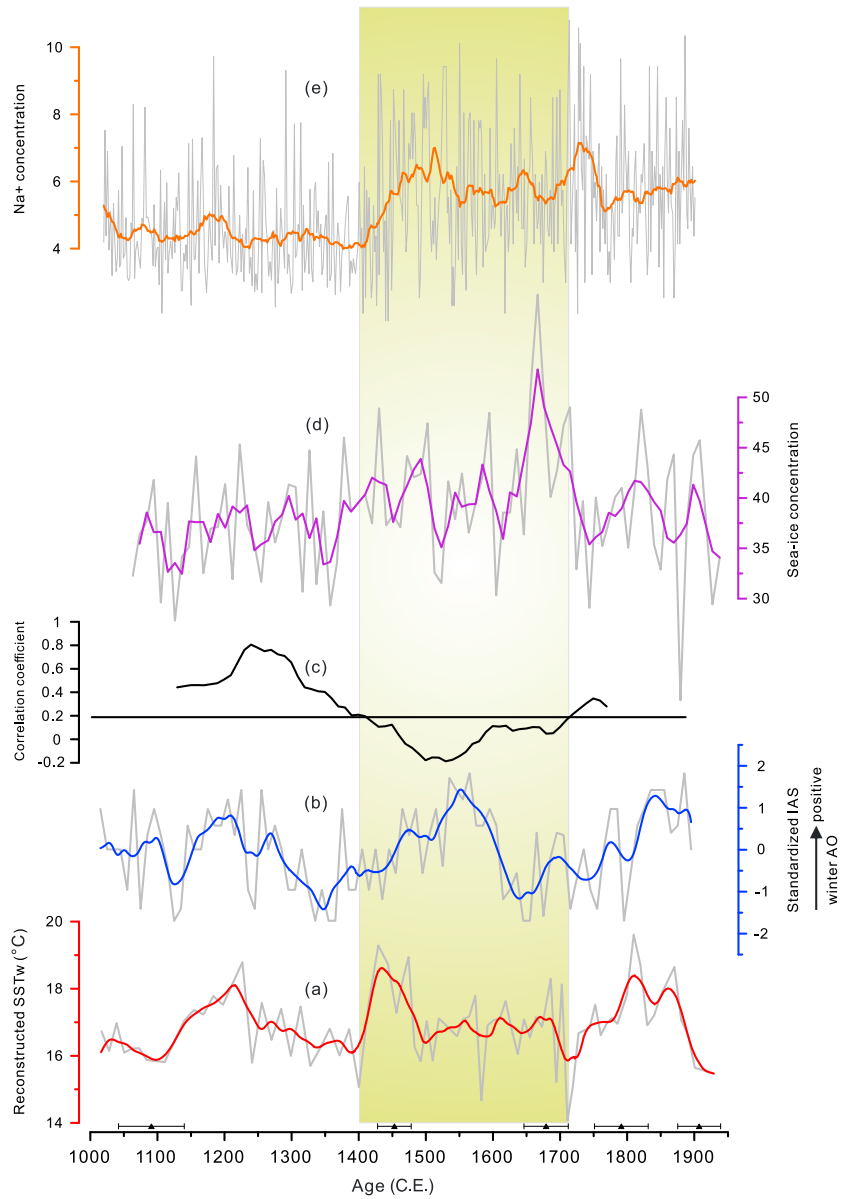


**Figure 7.** (a) The reconstructed SST<sub>w</sub> of core MD05-2908; (b) changes in the standardized IAS (index of abnormal snow) (Chu et al., 2008); (c) running correlation coefficient between SST<sub>w</sub> and the standardized IAS (calculated for moving 250 year windows); (d) sea ice concentration from core GA306-GC4, West Greenland (Sha et al., 2016), and (e) sea-salt ion (Na<sup>+</sup>) in the GISP2 ice core (Mayewski et al., 1997). Actual data are shown as gray curves; smoothed records (20 year running averages) are denoted by bold curves in color.

snow during winter” and “pray God for snow”) per decade, and PSE is the number of years with positive snow events per decade (defined from direct descriptions). The results show that the IAS is positively correlated with the AO signature in a coral time series from the Red Sea (Felis et al., 2004; Rimbu et al., 2001). Furthermore, the relationship between snow cover and the AO index from 1967 C.E. to 2000 C.E. was also examined by Bamzai (2003) based on satellite-derived global snow cover data on a weekly timescale. The results suggested that on a monthly timescale, the AO index during January, February, and March (JFM) is significantly correlated with snow cover in concurrent and subsequent spring months, particularly over Eurasia. On seasonal timescales, it was shown that JFM AO and JFM snow cover over Eurasia are significantly correlated ( $r = -0.49$ , significant at 99% level) (Bamzai, 2003). Vicente-Serrano et al. (2007) also found that the variability in the timing of snow cover disappearance was significantly related to the AO in western Siberia.

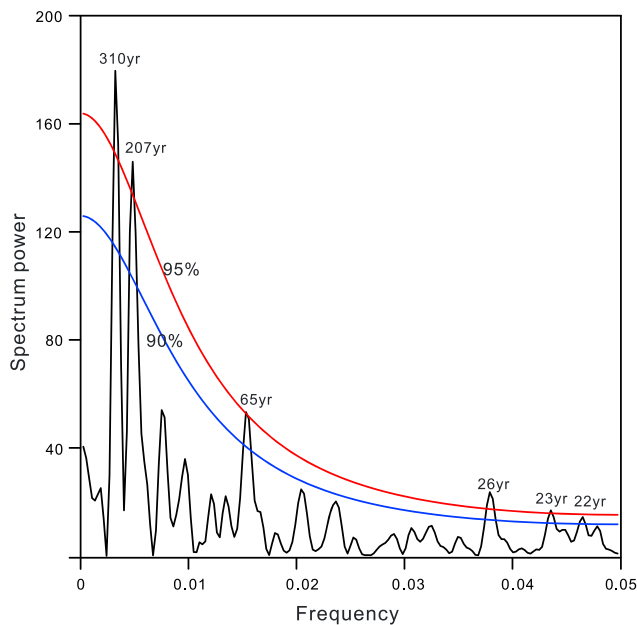


**Figure 8.** Results of spectral analysis of the reconstructed  $SST_w$  record from core MD05-2908. The colored lines indicate the 95% (red), and 90% (blue) false-alarm levels. Notable peaks occur at 310, 207, and 65 years (>95% false-alarm levels). Peaks at 26 years and below are too close to the Nyquist frequency to be reliable.

Consequently, Chu et al. (2008, 2012) and Lee et al. (2015) used the standardized IAS to infer winter AO variability over the past millennium.

To test the link between the AO and EAWM during the last millennium, we compared the reconstructed  $SST_w$  in our study with the standardized IAS in Eastern Asia (Chu et al., 2008) (Figures 7a and 7b). The correlation coefficients between  $SST_w$  and the IAS exceed 0.2 prior to ~1400 C.E., with even higher correlations, exceeding 0.6, during the interval 1200–1300 C.E. (Figure 7c). This suggests a coherent variability in the EAWM and winter AO between 1000 and 1400 C.E. Modern instrumental winter temperatures recorded in northern China also reveal a close link with the AO index between 1956 and 2005 C.E. (Feng et al., 2009).

According to Ma, Wang, and Zhang (2012) and Zhou and Wang (2014), the reduction in Arctic sea ice cover could potentially affect the overall climate of the Northern Hemisphere. Consequently, we also compared our  $SST_w$  in the southern Okinawa Trough with reconstructed Arctic sea ice records (Mayewski et al., 1997; Sha et al., 2016) during the last millennium (Figures 7d and 7e). The diatom-based sea ice concentration (SIC) reconstruction can be used to infer Arctic sea ice cover variability, which is supported by the good correlation between the reconstructed SIC and the satellite SIC data for the period 1979–2006 C.E. ( $r = 0.43$ ) (Sha et al., 2016). The concentration of sea-salt ion ( $Na^+$ ) in the Greenland Ice Sheet Project 2 (GISP2) ice core (Mayewski et al., 1997) (Figure 7e), which may be linked to sea surface windiness and/or sea ice openness (Kreutz et al., 1997; Mayewski, White, & Margulis, 2002), indicates dis-

tinctly low values between 1000 and 1400 C.E., but with slightly higher values at about 1200 C.E. A generally similar pattern is also shown by the reconstructed diatom-based sea ice concentration from core GA306-GC4, West Greenland, which records low sea ice concentrations from 1000 to 1400 C.E. (Sha et al., 2016) (Figure 7d). However, this record exhibits greater variability, possibly due to the impact of solar forcing and variations in ocean currents (Sha et al., 2016). The generally smaller extent of sea ice during the interval 1000–1400 C.E. coincides with the positive correlation between EAWM and winter AO (Figure 7c).

Compared to the positive correlation between EAWM and winter AO during the interval 1000–1400 C.E., there is no significant correlation between the EAWM and winter AO between 1400 and 1700 C.E., inferred by the very low and even negative correlation coefficient between the reconstructed  $SST_w$  and IAS (Figure 7c). At the same time, there was a distinct increase in sea ice as indicated both by high  $Na^+$  concentration in GISP2 and by the sea ice concentration in West Greenland during the interval 1400–1700 C.E. (Figures 7d and 7e), the coldest time period of the LIA. Thereafter, the link between EAWM and winter AO became stronger between 1750 and 1900 C.E., indicated by the increasing correlation coefficient between the reconstructed  $SST_w$  and IAS, coinciding with a general reduction in sea ice (Figures 7c–7e).

Our data therefore suggest that there is an unstable relationship between EAWM and AO on centennial time-scales and that these relationships may be different (and even opposite) during different time intervals. We suggest that Arctic sea ice cover plays an important role in linking the AO and the EAWM. During periods of more extensive sea ice, the East Asian jet stream is located further southwards, resulting in little contact with the Polar cell and the Siberian High. In contrast, during periods of reduced sea ice cover and surface warming over the Arctic, the changes in the meridional temperature gradient may lead to a westward penetration of the East Asian jet stream, strengthening the impact of the AO on the EAWM (Gao et al., 2015; Li et al., 2014). This pattern is also in accord with the positive correlation of the AO and the EAWM for the interval from 1983–2012 C.E., when there was an extensive reduction in Arctic sea ice. It also suggests that continued reduction of Arctic sea ice in the future may further strengthen the link between the EAWM and winter AO.

Spectral analysis of the detrended  $SST_w$  record in the southern Okinawa Trough over the last millennium reveals statistically significant (above the 95% confidence level), decadal-to-centennial periodicities centered at 310, 207, 65, and 26–22 years (Figure 8). However, the fluctuations with periods of ~22–26 years are

uncertain because they are close to the Nyquist frequency of the data set. The 207 year periodicity resolved in the diatom-based SST<sub>W</sub> reconstruction (Figure 8) is close to the ubiquitous 210 year <sup>14</sup>C and <sup>10</sup>Be cycle, known as the de Vries cycle (Abreu, Beer, & Ferriz-Mas, 2010; Steinhilber et al., 2012; Stuiver & Braziunas, 1993). This suggests that solar activity partly influences EAWM strength on a centennial timescale. A solar-EAWM linkage during the Holocene has also been proposed in several studies (Liu et al., 2009; Nakanishi et al., 2012; Sagawa et al., 2014; Xiao et al., 2006; Yang et al., 2015). In addition, the 65 year periodicity in the diatom-based SST<sub>W</sub> closely resembles the typical periodicities of the Atlantic Multidecadal Oscillation (AMO) (55–80 years) and the multidecadal variation of North Atlantic sea surface temperature (SST) (Delworth & Mann, 2000; Kerr, 2000; Knudsen et al., 2011), but may be uncertain because of the effects of dating uncertainties (Mudelsee, 2010, 2014; Mudelsee et al., 2009).

## 5. Conclusions

1. A high-resolution diatom record from core MD05-2908 from the southern Okinawa Trough reveals pronounced paleoceanographic changes in the area during the last millennium. We find a high degree of similarity between our diatom-based reconstruction of winter sea surface temperatures (SST<sub>W</sub>) for the past 500 years and a winter temperature index record based on historical documents from southern China, demonstrating that our proxy is reliable and can be used for longer time series.
2. Our SST reconstruction reveals relatively high SST<sub>W</sub> conditions during the intervals 1130–1250, 1400–1480, and 1750–1870 C.E., which were related to a weakening of the influence of the East Asian winter monsoon (EAWM). A strong EAWM during the intervals 1300–1400 and 1500–1750 C.E., as inferred by decreased SST<sub>W</sub> in the southern Okinawa Trough, corresponds well with historic evidence for a low frequency of warm winters.
3. The changes in the EAWM revealed by our SST<sub>W</sub> reconstruction correspond closely to the winter Arctic Oscillation (AO) inferred by the Index of Abnormal Snow (IAS) during the interval 1000–1400 C.E., associated with a reduction in Arctic sea ice. However, there is no significant correlation between the EAWM and winter AO between 1400 and 1750 C.E. when Arctic sea ice increased. This suggests that Arctic sea ice cover plays a key role in determining the relationship between the EAWM and winter AO, and with the ongoing reduction of Arctic sea ice it may strengthen the relationship between the AO and EAWM in the future.
4. Spectral analysis results suggest that the solar activity and potentially also the Atlantic Multidecadal Oscillation (AMO) may also be forcing mechanisms of variations in East China Sea oceanography and SST, although the latter lies within the age uncertainty range.

### Acknowledgments

We are grateful to the Institute Paul-Emil Victor (IPEV) for the Marco Polo 2 IMAGES coring operation onboard the R/V *Marion Dufresne* in 2005. We also thank the shipboard party and the captain and crew of the *Marion Dufresne* for their hard work in obtaining the core used in this study. Financial support for this work was provided by the National Natural Science Foundation of China (grants 41302134, 41406209, 41176048, 41230959, 41476043, 41776193, and U1609203), the Natural Science Foundation of Zhejiang Province (grants LY17D060001 and LQ15D20001), the Chinese Polar Environment Comprehensive Investigation and Assessment Programs (grant CHINARE2017-03-02), Strategic Priority Research Program of the Chinese Academy of Sciences (A) (grant XDA11030104), National Program on Global Change and Air-Sea Interaction (grants GASI-GEOGE-06-02 and GASI-GEOGE-04), and K.C. Wong Magna Fund in Ningbo University. Finally, we thank Ellen Thomas, Ryuji Tada, Kuo-Yen Wei, and one anonymous reviewer for their constructive and useful comments. The reconstructed SST<sub>W</sub> data used in this study can be found in the supporting information.

## References

- Abreu, J. A., Beer, J., & Ferriz-Mas, A. (2010). Past and future solar activity from cosmogenic radionuclides. In S. R. Cranmer, J. T. Hoeksema, & J. L. Kohl (Eds.), *SOHO-23: Understanding a peculiar solar minimum*. *Astronomical Society of the Pacific Conference Series* (Vol. 428, pp. 287–295). San Francisco, CA: Astronomical Society of the Pacific.
- Arakawa, H. (1954). Fujiwhara on five centuries of freezing dates of Lake Suwa in the central Japan. *Theoretical and Applied Climatology*, 6(1), 152–166.
- Bamzai, A. S. (2003). Relationship between snow cover variability and Arctic oscillation index on a hierarchy of time scales. *International Journal of Climatology*, 23(2), 131–142. <https://doi.org/10.1002/joc.854>
- Bard, E., Raisbeck, G., Yiou, F., & Jouzel, J. (2000). Solar irradiance during the last 1200 years based on cosmogenic nuclides. *Tellus B*, 52(3), 985–992. <https://doi.org/10.3402/tellusb.v52i3.17080>
- Belt, S. T., Massé, G., Rowland, S. J., Poulin, M., Michel, C., & LeBlanc, B. (2007). A novel chemical fossil of palaeo sea ice: IP25. *Organic Geochemistry*, 38, 16–27. <https://doi.org/10.1016/j.orggeochem.2006.09.013>
- Berner, K. S., Koç, N., Divine, D., Godtlielbsen, F., & Moros, M. (2008). A decadal-scale Holocene sea surface temperature record from the subpolar North Atlantic constructed using diatoms and statistics and its relation to other climate parameters. *Paleoceanography*, 23, PA2210. <https://doi.org/10.1029/2006PA001339>
- Bickert, T., & Wefer, G. (1999). South Atlantic and benthic foraminifer  $\delta^{13}\text{C}$  deviations: Implications for reconstructing the late Quaternary deep-water circulation. *Deep-Sea Research Part II*, 46(1–2), 437–452. [https://doi.org/10.1016/S0967-0645\(98\)00098-8](https://doi.org/10.1016/S0967-0645(98)00098-8)
- Birks, C. J. A., & Koç, N. (2002). A high-resolution diatom record of late-Quaternary sea-surface temperatures and oceanographic conditions from the eastern Norwegian Sea. *Boreas*, 31(4), 323–344. <https://doi.org/10.1080/030094802320942545>
- Chang, Y., Wang, W., Yokoyama, Y., Matsuzaki, H., Kawahata, H., & Chen, M. (2008). Millennial-scale planktic foraminifer faunal variability in the East China Sea during the past 40000 years (IMAGES MD012404 from the Okinawa Trough). *Terrestrial, Atmospheric and Oceanic Sciences*, 19, 389–401. [https://doi.org/10.3319/TAO.2008.19.4.389\(IMAGES\)](https://doi.org/10.3319/TAO.2008.19.4.389(IMAGES))
- Chu, G., Sun, Q., Wang, X., & Sun, J. (2008). Snow anomaly events from historical documents in eastern China during the past two millennia and implication for low-frequency variability of AO/NAO and PDO. *Geophysical Research Letters*, 35, L14806. <https://doi.org/10.1029/2008GL034475>

- Chu, G., Sun, Q., Wang, X., Liu, M., Lin, Y., Xie, M., ... Liu, J. (2012). Seasonal temperature variability during the past 1600 years recorded in historical documents and varved lake sediment profiles from northeastern China. *Holocene*, 22, 785–792. <https://doi.org/10.1177/0959683611430413>
- Crosta, X., Pichon, J. J., & Burckle, L. H. (1998). Application of modern analog technique to marine Antarctic diatoms: Reconstruction of maximum sea-ice extent at the Last Glacial Maximum. *Paleoceanography*, 13(3), 284–297. <https://doi.org/10.1029/98PA00339>
- D'Arrigo, R., Frank, D., Jacoby, G., & Pederson, N. (2001). Spatial response to major volcanic events in or about AD 536, 934 and 1258: Frost rings and other dendrochronological evidence from Mongolia and northern Siberia: Comment on RB Stothers, 'Volcanic dry fogs, climate cooling, and plague pandemics in Europe and the Middle East' (Climatic Change, 42, 1999). *Climatic Change*, 49(1), 239–246.
- D'Arrigo, R., Wilson, R., Panagiotopoulos, F., & Wu, B. (2005). On the long-term interannual variability of the east Asian winter monsoon. *Geophysical Research Letters*, 32, 97–116. <https://doi.org/10.1029/2005GL023235>
- Delworth, T. L., & Mann, M. E. (2000). Observed and simulated multidecadal variability in the Northern Hemisphere. *Climate Dynamics*, 16(9), 661–676. <https://doi.org/10.1007/s003820000075>
- Diekmann, B., Hofmann, J., Henrich, R., Fütterer, D. K., Röhl, U., & Wei, K. (2008). Detrital sediment supply in the southern Okinawa Trough and its relation to sea-level and Kuroshio dynamics during the late Quaternary. *Marine Geology*, 255, 83–95. <https://doi.org/10.1016/j.margeo.2008.08.001>
- Dou, Y., Yang, S., Liu, Z., Cliff, P. D., Yu, H., Berne, S., & Shi, X. (2010). Clay mineral evolution in the central Okinawa Trough since 28 ka: Implications for sediment provenance and paleoenvironmental change. *Palaeogeography Palaeoclimatology Palaeoecology*, 288, 108–117. <https://doi.org/10.1016/j.palaeo.2010.01.040>
- Dykoski, C. A., Edwards, R. L., Cheng, H., Yuan, D., Cai, Y., Zhang, M., ... Revenaugh, J. (2005). A high-resolution, absolute-dated Holocene and deglacial Asian monsoon record from Dongge Cave, China. *Earth and Planetary Science Letters*, 233, 71–86. <https://doi.org/10.1016/j.epsl.2005.01.036>
- Ebisuzaki, W. (1997). A method to estimate the statistical significance of a correlation when the data are serially correlated. *Journal of Climate*, 10(9), 2147–2153. [https://doi.org/10.1175/1520-0442\(1997\)010%3C2147:AMTETS%3E2.0.CO;2](https://doi.org/10.1175/1520-0442(1997)010%3C2147:AMTETS%3E2.0.CO;2)
- Fan, K., & Wang, H. (2004). Antarctic oscillation and the dust weather frequency in North China. *Geophysical Research Letters*, 31, L10201. <https://doi.org/10.1029/2004GL019465>
- Fan, K., & Wang, H. (2006). Interannual variability of Antarctic Oscillation and its influence on East Asian climate during boreal winter and spring. *Science China Earth Sciences*, 49, 554–560. <https://doi.org/10.1007/s11430-006-0554-7>
- Felis, T., Lohmann, G., Kuhnert, H., Lorenz, S. J., Scholz, D., Pätzold, J., ... Al-Moghrabi, S. M. (2004). Increased seasonality in Middle East temperatures during the last interglacial period. *Nature*, 429, 164–168. <https://doi.org/10.1038/nature02546>
- Feng, S., Gong, D., Zhang, Z., He, X., Guo, D., & Lei, Y. (2009). Wind-chill temperature changes in winter over China during the last 50 years (in Chinese with English abstract). *Acta Geographica Sinica*, 64, 1071–1082.
- Gao, Y., Sun, J., Li, F., He, S., Sandven, S., Yan, Q., ... Furevik, T. (2015). Arctic sea ice and Eurasian climate: A review (in Chinese with English abstract). *Advances in Atmospheric Sciences*, 32(1), 92–114. <https://doi.org/10.1007/s00376-014-0009-6>
- Gong, D., & Ho, C. (2002). The Siberian High and climate change over middle to high latitude Asia. *Theoretical and Applied Climatology*, 72(1–2), 1–9. <https://doi.org/10.1007/s007040200008>
- Gong, D., Wang, S., & Zhu, J. (2001). East Asian winter monsoon and Arctic oscillation. *Geophysical Research Letters*, 28(10), 2073–2076. <https://doi.org/10.1029/2000GL012311>
- Hadley Centre for Climate Prediction and Research (2007): HadISST1.1—Global monthly mean gridded SSTs (1870–2015). NCAS British Atmospheric Data Centre.
- Håkansson, H. (1984). The recent diatom succession of Lake Havgårdssjöön, south Sweden. In D. G. Mann (Ed.), *Proceeding of the Seventh International Diatom Symposium* (pp. 411–429). Philadelphia: Otto Koeltz.
- Hantemirov, R. M., & Shiyatov, S. G. (2002). A continuous multimillennial ring-width chronology in Yamal, northwestern Siberia. *Holocene*, 12(6), 717–726. <https://doi.org/10.1191/0959683602hl585rp>
- He, S., & Wang, H. (2013a). Oscillating relationship between the East Asian winter monsoon and ENSO. *Journal of Climate*, 26(24), 9819–9838. <https://doi.org/10.1175/JCLI-D-13-00174.1>
- He, S., & Wang, H. (2013b). Impact of the November/December Arctic Oscillation on the following January temperature in East Asia. *Journal of Geophysical Research: Atmospheres*, 118, 12,981–12,998. <https://doi.org/10.1002/2013JD020525>
- Hideshima, S., Matsumoto, E., Abe, O., & Kitagawa, H. (2001). Northwest Pacific marine reservoir correction estimated from annually banded coral from Ishigaki Island, southern Japan. *Radiocarbon*, 43(2A), 473–476. <https://doi.org/10.1017/S0033822200038352>
- Hu, C., Henderson, G. M., Huang, J., Xie, S., Sun, Y., & Johnson, K. R. (2008). Quantification of Holocene Asian monsoon rainfall from spatially separated cave records. *Earth and Planetary Science Letters*, 266, 221–232. <https://doi.org/10.1016/j.epsl.2007.10.015>
- Hu, B., Yang, Z., Zhao, M., Saito, Y., Fan, D., & Wang, L. (2012). Grain size records reveal variability of the East Asian Winter Monsoon since the middle Holocene in the Central Yellow Sea mud area, China. *Science China Earth Sciences*, 55, 1656–1668. <https://doi.org/10.1007/s11430-012-4447-7>
- Huang, Y., Jiang, H., Björck, S., Li, T., Lu, H., & Ran, L. (2009). Surface sediment diatoms from the western Pacific marginal seas and their correlation to environmental variables. *Chinese Journal of Oceanology and Limnology*, 27, 674–682. <https://doi.org/10.1007/s00343-009-9211-2>
- Jensen, K. G., Kuijpers, A., Koç, N., & Heinemeier, J. (2004). Diatom evidence of hydrographic changes and ice conditions in Igaliku Fjord, South Greenland, during the past 1500 years. *Holocene*, 14, 152–164. <https://doi.org/10.1191/0959683604hl698rp>
- Jian, Z., Wang, P., Saito, Y., Wang, J., Pflaumann, U., Oba, T., & Cheng, X. (2000). Holocene variability of the Kuroshio Current in the Okinawa Trough, northwestern Pacific Ocean. *Earth and Planetary Science Letters*, 184(1), 305–319. [https://doi.org/10.1016/S0012-821X\(00\)00321-6](https://doi.org/10.1016/S0012-821X(00)00321-6)
- Jiang, H., Zheng, Y., Ran, L., & Seidenkrantz, M.-S. (2004). Diatoms from the surface sediments of the South China Sea and their relationships to modern hydrography. *Marine Micropaleontology*, 53(3–4), 279–292. <https://doi.org/10.1016/j.marmicro.2004.06.005>
- Jiang, H., Muscheler, R., Björck, S., Seidenkrantz, M.-S., Olsen, J., Sha, L., ... Knudsen, M. F. (2015). Solar forcing of Holocene summer sea-surface temperatures in the northern North Atlantic. *Geology*, 43(3), 203–206. <https://doi.org/10.1130/G36377.1>
- Juggins, S. (2003). *C2 User Guide: Software for Ecological and Palaeoecological Data Analysis and Visualisation. Version 1.5*. Newcastle University: Newcastle upon Tyne.
- Justwan, A., & Koç, N. (2008). A diatom based transfer function for reconstructing sea ice concentrations in the North Atlantic. *Marine Micropaleontology*, 66, 264–278. <https://doi.org/10.1016/j.marmicro.2007.11.001>
- Kanaya, T., & Koizumi, I. (1966). Interpretation of diatom thanatocoenoses from the North Pacific applied to a study of core V20-130 (studies of a deep-sea core V20-130, part IV). *Science reports of the Research Institute, Tohoku University. Series A: Physics*, 2(37), 89–130.

- Kao, S., Dai, M., Wei, K., Blair, N. E., & Lyons, W. B. (2008). Enhanced supply of fossil organic carbon to the Okinawa Trough since the last deglaciation. *Paleoceanography*, 23, PA2207. <https://doi.org/10.1029/2007PA001440>
- Keigwin, L. (1996). The Little Ice Age and Medieval Warm Period in the Sargasso Sea. *Science*, 274(5292), 1503–1508. <https://doi.org/10.1126/science.274.5292.1503>
- Kerr, R. (2000). A North Atlantic climate pacemaker for the centuries. *Science*, 288(5473), 1984–1985. <https://doi.org/10.1126/science.288.5473.1984>
- Knudsen, M. F., Seidenkrantz, M.-S., Jacobsen, B. H., & Kuijpers, A. (2011). Tracking the Atlantic Multidecadal Oscillation through the last 8,000 years. *Nature Communications*, 2, 178. <https://doi.org/10.1038/ncomms1186>
- Koc, N., & Schrader, H. (1990). Surface sediment diatom distribution and Holocene Paleotemperature variations in the Greenland, Iceland and Norwegian Sea. *Paleoceanography*, 5, 557–580.
- Koizumi, I., Tada, R., Narita, H., Irino, T., Aramaki, T., Oba, T., & Yamamoto, H. (2006). Paleoceanographic history around the Tsugaru Strait between the Japan Sea and the Northwest Pacific Ocean since 30 cal kyr BP. *Palaeogeography Palaeoclimatology Palaeoecology*, 232, 36–52. <https://doi.org/10.1016/j.palaeo.2005.09.003>
- Krawczyk, D. W., Witkowski, A., Moros, M., Lloyd, J. M., Kuijpers, A., & Kierzek, A. (2010). Late-Holocene diatom-inferred reconstruction of temperature variations of the West Greenland Current from Disko Bugt, central West Greenland. *Holocene*, 20, 659–666. <https://doi.org/10.1177/0959683610371993>
- Krawczyk, D. W., Witkowski, A., Moros, M., Lloyd, J. M., Høyer, J. L., Miettinen, A., & Kuijpers, A. (2017). Quantitative reconstruction of Holocene sea ice and sea surface temperature off West Greenland from the first regional diatom data set. *Paleoceanography*, 32, 18–40. <https://doi.org/10.1002/2016PA003003>
- Kreutz, K., Mayewski, P., Meeker, L., Twickler, M., Whitlow, S., & Pittalwala, I. (1997). Bipolar changes in atmospheric circulation during the Little Ice Age. *Science*, 277(5330), 1294–1296. <https://doi.org/10.1126/science.277.5330.1294>
- Kubota, Y., Kimoto, K., Tada, R., Oda, H., Yokoyama, Y., & Matsuzaki, H. (2010). Variations of East Asian summer monsoon since the last deglaciation based on  $\delta^{18}O$  and oxygen isotope of planktic foraminifera in the northern East China Sea. *Paleoceanography*, 25, PA4205. <https://doi.org/10.1029/2009PA001891>
- Kubota, Y., Tada, R., & Kimoto, K. (2015). Changes in East Asian summer monsoon precipitation during the Holocene deduced from a freshwater flux reconstruction of the Changjiang (Yangtze River) based on the oxygen isotope mass balance in the northern East China Sea. *Climate of the Past*, 11(2), 265–281. <https://doi.org/10.5194/cp-11-265-2015>
- Lau, N.-C., & Nath, M. J. (2000). Impact of ENSO on the variability of the Asian-Australian monsoons as simulated in GCM experiments. *Journal of Climate*, 13(24), 4287–4309. [https://doi.org/10.1175/1520-0442\(2000\)013<4287:IOEOTV>2.0.CO;2](https://doi.org/10.1175/1520-0442(2000)013<4287:IOEOTV>2.0.CO;2)
- Lee, H., & Chao, S. (2003). A climatological description of circulation in and around the East China Sea. *Deep-Sea Research Pt. II*, 50(6-7), 1065–1084. [https://doi.org/10.1016/S0967-0645\(03\)00010-9](https://doi.org/10.1016/S0967-0645(03)00010-9)
- Lee, H. F., Pei, Q., Zhang, D. D., & Choi, K. P. (2015). Quantifying the intra-regional precipitation variability in northwestern China over the past 1,400 years. *PLoS One*, 10(7), e0131693. <https://doi.org/10.1371/journal.pone.0131693>
- Li, S., & Bates, G. T. (2007). Influence of the Atlantic Multidecadal Oscillation on the winter climate of East China. *Advances in Atmospheric Sciences*, 24, 126–135. <https://doi.org/10.1007/s00376-007-0126-6>
- Li, F., & Wang, H. (2013a). Relationship between Bering Sea ice cover and East Asian winter monsoon year-to-year variations. *Advances in Atmospheric Sciences*, 30(1), 48–56. <https://doi.org/10.1007/s00376-012-2071-2>
- Li, F., & Wang, H. (2013b). Spring surface cooling trend along the East Asian coast after the late 1990s. *Chinese Science Bulletin*, 58(31), 3847–3851. <https://doi.org/10.1007/s11434-013-5853-8>
- Li, F., & Wang, H. (2014). Autumn Eurasian snow depth, autumn Arctic sea ice cover and East Asian winter monsoon. *International Journal of Climatology*, 34(13), 3616–3625. <https://doi.org/10.1002/joc.3936>
- Li, B., Jian, Z., & Wang, P. (1997). *Pulleniatina obliquiloculata* as a paleoceanographic indicator in the southern Okinawa Trough during the last 20,000 years. *Marine Micropaleontology*, 32(1–2), 59–69.
- Li, T., Liu, Z., Hall, M. A., Berne, S., Saito, Y., Cang, S., & Cheng, Z. (2001). Heinrich event imprints in the Okinawa Trough: Evidence from oxygen isotope and planktonic foraminifera. *Palaeogeography Palaeoclimatology Palaeoecology*, 176(1–4), 133–146. [https://doi.org/10.1016/S0031-0182\(01\)00332-7](https://doi.org/10.1016/S0031-0182(01)00332-7)
- Li, C., Jiang, B., Li, A., Li, T., & Jiang, F. (2009). Sedimentation rates and provenance analysis in the southwestern Okinawa Trough since the mid-Holocene. *Chinese Science Bulletin*, 54, 1234–1242.
- Li, D., Kundsén, M. F., Jiang, H., Olsen, J., Zhao, M., Li, T., ... Sha, L. (2012). A diatom-based reconstruction of summer sea-surface salinity in the southern Okinawa Trough, East China Sea, over the last millennium. *Journal of Quaternary Science*, 27, 771–779. <https://doi.org/10.1002/jqs.2562>
- Li, F., Wang, H., & Gao, Y. (2014). On the strengthened relationship between the East Asian Winter Monsoon and Arctic Oscillation: A comparison of 1950–70 and 1983–2012. *Journal of Climate*, 27(13), 5075–5091. <https://doi.org/10.1175/JCLI-D-13-00335.1>
- Li, H.-C., Zhao, M., Tsai, C.-H., Mii, H.-S., Chang, Q., & Wei, K.-Y. (2015). The first high-resolution stalagmite record from Taiwan: Climate and environmental changes during the past 1300 years. *Journal of Asian Earth Sciences*, 114(3), 574–587. <https://doi.org/10.1016/j.jseaes.2015.07.025>
- Lin, Y., Wei, K., Lin, I., Yu, P., Chiang, H., Chen, C., ... Chen, Y. (2006). The Holocene Pulleniatina Minimum Event revisited: Geochemical and faunal evidence from the Okinawa Trough and upper reaches of the Kuroshio current. *Marine Micropaleontology*, 59, 153–170. <https://doi.org/10.1016/j.marmicro.2006.02.003>
- Liu, X., Dong, H., Yang, X., Herzsich, U., Zhang, E., Stuet, J.-B. W., & Wang, Y. (2009). Late Holocene forcing of the Asian winter and summer monsoon as evidenced by proxy records from the northern Qinghai-Tibetan Plateau. *Earth and Planetary Science Letters*, 280, 276–284. <https://doi.org/10.1016/j.epsl.2009.01.041>
- Liu, Y., Sha, L., Shi, X., Suk, B. C., Li, C., Wang, K., & Li, X. (2010). Depositional environment in the southern Ulleung Basin, East Sea (Sea of Japan), during the last 48000 years. *Acta Oceanologica Sinica*, 29, 52–64. <https://doi.org/10.1007/s13131-010-0063-6>
- Liu, J., Curry, J. A., Wang, H., Song, M., & Horton, R. M. (2012). Impact of declining Arctic sea ice on winter snowfall. *Proceedings of the National Academy of Sciences of the United States of America*, 109, 4074–4079. <https://doi.org/10.1073/pnas.1114910109>
- Lomb, N. R. (1976). Least-squares frequency analysis of unequally spaced data. *Astrophysics and Space Science*, 39(2), 447–462. <https://doi.org/10.1007/BF00648343>
- Ma, J., Wang, H., & Zhang, Y. (2012). Will boreal winter precipitation over China increase in the future? An AGCM simulation under summer “ice-free Arctic” conditions. *Chinese Science Bulletin*, 57, 921–926. <https://doi.org/10.1007/s11434-011-4925-x>
- Magnuson, J. J., Robertson, D. M., Benson, B. J., Wynne, R. H., Livingstone, D. M., Arai, T., ... Vuglinski, V. S. (2000). Historical trends in lake and river ice cover in the Northern Hemisphere. *Science*, 289(5485), 1743–1746. <https://doi.org/10.1126/science.289.5485.1743>

- Mayewski, P. A., Meeker, L. D., Twickler, M. S., Whitlow, S., Yang, Q., Lyons, W. B., & Prentice, M. (1997). Major features and forcing of high-latitude northern hemisphere atmospheric circulation using a 110,000-year-long glaciochemical series. *Journal of Geophysical Research*, 102(C12), 26,345–26,366. <https://doi.org/10.1029/96JC03365>
- Mayewski, P. A., White, F., & Margulis, L. (2002). *The ice chronicles: The quest to understand global climate change*. Hanover: University of New Hampshire Press.
- Miettinen, A., Koç, N., Hall, I. R., Godtlibsen, F., & Divine, D. (2011). North Atlantic sea surface temperatures and their relation to the North Atlantic Oscillation during the last 230 years. *Climate Dynamics*, 36, 533–543. <https://doi.org/10.1007/s00382-010-0791-5>
- Miller, K. R., Chapman, M. R., Andrews, J. E., & Koç, N. (2011). Diatom phytoplankton response to Holocene climate change in the Subpolar North Atlantic. *Global and Planetary Change*, 79, 214–225. <https://doi.org/10.1016/j.gloplacha.2011.03.001>
- Mudelsee, M. (2010). *Climate time series analysis: Classical statistical and bootstrap methods*. Dordrecht, Heidelberg, London, New York: Springer. <https://doi.org/10.1007/978-90-481-9482-7>
- Mudelsee, M. (2014). *Climate time series analysis: Classical statistical and bootstrap methods* (2nd ed.). Cham, Heidelberg, New York, Dordrecht, London: Springer. <https://doi.org/10.1007/978-3-319-04450-7>
- Mudelsee, M., Scholz, D., Röthlisberger, R., Fleitmann, D., Mangini, A., & Wolff, E. W. (2009). Climate spectrum estimation in the presence of timescale errors. *Nonlinear Processes in Geophysics*, 16, 43–56. <https://doi.org/10.5194/npg-16-43-2009>
- Müller, J., Massé, G., Stein, R., & Simon, T. (2009). Variability of sea-ice conditions in the Fram Strait over the past 30,000 years. *Nature Geoscience*, 2, 772–776. <https://doi.org/10.1038/ngeo665>
- Nakanishi, T., Yamamoto, M., Tada, R., & Oda, H. (2012). Centennial-scale winter monsoon variability in the northern East China Sea during the Holocene. *Journal of Quaternary Science*, 27, 956–963. <https://doi.org/10.1002/jqs.2589>
- Naurzbaev, M. M., Vaganov, E. A., Sidorova, O. V., & Schweingruber, F. H. (2002). Summer temperatures in eastern Taimyr inferred from a 2427-year late-Holocene tree-ring chronology and earlier floating series. *Holocene*, 12(6), 727–736. <https://doi.org/10.1191/0959683602hl586rp>
- Nyberg, J., Malmgren, B. A., Kuijpers, A., & Winter, A. (2002). A centennial-scale variability of tropical North Atlantic surface hydrography during the late Holocene. *Palaeoogeography Palaeoecology*, 183(1–2), 25–41. [https://doi.org/10.1016/S0031-0182\(01\)00446-1](https://doi.org/10.1016/S0031-0182(01)00446-1)
- Peltier, W. R., & Fairbanks, R. G. (2006). Global glacial ice volume and Last Glacial Maximum duration from an extended Barbados sea level record. *Quaternary Science Reviews*, 25, 3322–3337. <https://doi.org/10.1016/j.quascirev.2006.04.010>
- Ramsey, C. B. (2008). Deposition models for chronological records. *Quaternary Science Reviews*, 27, 42–60. <https://doi.org/10.1016/j.quascirev.2007.01.019>
- Rayner, N. A., Parker, D. E., Horton, E. B., Folland, C. K., Alexander, L. V., Rowell, D. P., ... Kaplan, A. (2003). Global analyses of sea surface temperature, sea ice, and night marine air temperature since the late nineteenth century. *Journal of Geophysical Research*, 108(D14), 4407. <https://doi.org/10.1029/2002JD002670>
- Reimer, P. J., Baillie, M. G., Bard, E., Bayliss, A., Beck, J. W., Blackwell, P. G., ... Edwards, R. L. (2009). IntCal09 and Marine09 radiocarbon age calibration curves, 0–50,000 years cal BP. *Radiocarbon*, 51, 1111–1150. <https://doi.org/10.1017/S0033822200034202>
- Rimbu, N., Lohmann, G., Felis, T., & Patzold, J. (2001). Arctic Oscillation signature in a Red Sea coral. *Geophysical Research Letters*, 28(15), 2959–2962. <https://doi.org/10.1029/2001GL013083>
- Ruan, J., Xu, Y., Ding, S., Wang, Y., & Zhang, X. (2015). A high resolution record of sea surface temperature in southern Okinawa Trough for the past 15,000 years. *Palaeoogeography Palaeoecology*, 426, 209–215. <https://doi.org/10.1016/j.palaeo.2015.03.007>
- Sagawa, T., Kuwae, M., Tsuruoka, K., Nakamura, Y., Ikehara, M., & Murayama, M. (2014). Solar forcing of centennial-scale East Asian winter monsoon variability in the mid- to late Holocene. *Earth and Planetary Science Letters*, 395, 124–135. <https://doi.org/10.1016/j.epsl.2014.03.043>
- Salisbury, J., & Wimbush, M. (2002). Using modern time series analysis techniques to predict ENSO events from the SOI time series. *Nonlinear Processes in Geophysics*, 9(3/4), 341–345. <https://doi.org/10.5194/npg-9-341-2002>
- Scargle, J. D. (1982). Studies in astronomical time series analysis. II—Statistical aspects of spectral analysis of unevenly spaced data. *The Astrophysical Journal*, 263(2), 835–853. <https://doi.org/10.1086/160554>
- Schulz, M., & Mudelsee, M. (2002). REDFIT: Estimating red-noise spectra directly from unevenly spaced paleoclimatic time series. *Computational Geosciences*, 28(3), 421–426. [https://doi.org/10.1016/S0098-3004\(01\)00044-9](https://doi.org/10.1016/S0098-3004(01)00044-9)
- Sha, L., Jiang, H., Seidenkrantz, M.-S., Knudsen, K. L., Olsen, J., Kuijpers, A., & Liu, Y. (2014). A diatom-based sea-ice reconstruction for the Vaigat Strait (Disko Bugt, West Greenland) over the last 5000 yr. *Palaeoogeography Palaeoecology*, 403, 66–79. <https://doi.org/10.1016/j.palaeo.2014.03.028>
- Sha, L., Jiang, H., Seidenkrantz, M.-S., Muscheler, R., Zhang, X., Knudsen, M. F., ... Zhang, W. (2016). Solar forcing as an important trigger for West Greenland sea-ice variability over the last millennium. *Quaternary Science Reviews*, 131, 148–156. <https://doi.org/10.1016/j.quascirev.2015.11.002>
- Sha, L., Jiang, H., Seidenkrantz, M.-S., Li, D., Andresen, C. S., Knudsen, K. L., ... Zhao, M. (2017). A record of Holocene sea-ice variability off West Greenland and its potential forcing factors. *Palaeoogeography Palaeoecology*, 475, 115–124. <https://doi.org/10.1016/j.palaeo.2017.03.022>
- Steinhilber, F., Abreu, J. A., Beer, J., Brunner, I., Christl, M., Fischer, H., ... Wilhelms, F. (2012). 9400 years of cosmic radiation and solar activity from ice cores and tree rings. *Proceedings of the National Academy of Sciences of the United States of America*, 109(16), 5967–5971. <https://doi.org/10.1073/pnas.1118965109>
- Stothers, R. (2000). Climatic and demographic consequences of the massive volcanic eruption of 1258. *Climatic Change*, 45(2), 361–374. <https://doi.org/10.1023/A:1005523330643>
- Stuiver, M., & Braziunas, T. F. (1993). Sun, ocean, climate and atmospheric <sup>14</sup>CO<sub>2</sub>: An evaluation of causal and spectral relationships. *Holocene*, 3(4), 289–305. <https://doi.org/10.1177/095968369300300401>
- Stuiver, M., & Grootes, P. M. (2000). GISP2 oxygen isotope ratios. *Quaternary Research*, 53(03), 277–284. <https://doi.org/10.1006/qres.2000.2127>
- Stuiver, M., & Quay, P. D. (1980). Changes in atmospheric carbon-14 attributed to a variable Sun. *Science*, 207(4426), 11–19. <https://doi.org/10.1126/science.207.4426.11>
- Sun, Y., Oppo, D., Xiang, R., Liu, W., & Gao, S. (2005). Last deglaciation in the Okinawa Trough: Subtropical northwest Pacific link to Northern Hemisphere and tropical climate. *Paleoceanography*, 20, PA4005. <https://doi.org/10.1029/2004PA001061>
- ter Braak, C. J. F., & Smilauer, P. (2002). *CANOCO reference manual and canodraw for windows user's guide: software for canonical community ordination (version 4.5)* (p. 500). Ithaca, New York: Microcomputer Power.
- Tian, J., Huang, E., & Pak, D. K. (2010). East Asian winter monsoon variability over the last glacial cycle: Insights from a latitudinal sea-surface temperature gradient across the South China Sea. *Palaeoogeography Palaeoecology*, 292, 319–324. <https://doi.org/10.1016/j.palaeo.2010.04.005>

- Ujiie, H., Hatakeyama, Y., Gu, X. X., Yamamoto, S., Ishiwatari, R., & Maeda, L. (2001). Upward decrease of organic C/N ratios in the Okinawa Trough cores: Proxy for tracing the post-glacial retreat of the continental shore line. *Palaeoogeography Palaoclimatology Palaecology*, 165(1-2), 129–140. [https://doi.org/10.1016/S0031-0182\(00\)00157-7](https://doi.org/10.1016/S0031-0182(00)00157-7)
- de Vernal, A., Gersonde, R., Goosse, H., Seidenkrantz, M.-S., & Wolff, E. W. (2013). Sea ice in the paleoclimate system: The challenge of reconstructing sea ice from proxies—an introduction. *Quaternary Science Reviews*, 79, 1–8. <https://doi.org/10.1016/j.quascirev.2013.08.009>
- Versteegh, G. J., & Zonneveld, K. A. (2002). Use of selective degradation to separate preservation from productivity. *Geology*, 30(7), 615–618. [https://doi.org/10.1130/0091-7613\(2002\)030%3C0615:UOSDTS%3E2.0.CO;2](https://doi.org/10.1130/0091-7613(2002)030%3C0615:UOSDTS%3E2.0.CO;2)
- Vicente-Serrano, S. M., Grippa, M., Toan, T. L., & Mognard, N. (2007). Role of atmospheric circulation with respect to the interannual variability in the date of snow cover disappearance over northern latitudes between 1988 and 2003. *Journal of Geophysical Research*, 112, D08108. <https://doi.org/10.1029/2005JD006571>
- Walland, D., & Simmonds, I. (1996). Modelled atmospheric response to changes in Northern Hemisphere snow cover. *Climate Dynamics*, 13(1), 25–34. <https://doi.org/10.1007/s003820050150>
- Wang, H., & He, S. (2012). Weakening relationship between East Asian winter monsoon and ENSO after mid-1970s. *Chinese Science Bulletin*, 57, 3535–3540. <https://doi.org/10.1007/s11434-012-5285-x>
- Wang, Y., Cheng, H., Edwards, R. L., He, Y., Kong, X., An, Z., ... Li, X. (2005). The Holocene Asian monsoon: Links to solar changes and North Atlantic climate. *Science*, 308, 854–857. <https://doi.org/10.1126/science.1106296>
- Wang, B., Huang, F., Wu, Z., Yang, J., Fu, X., & Kikuchi, K. (2009). Multiscale climate variability of the South China Sea monsoon: A review. *Dynamics of Atmospheres and Oceans*, 47, 15–37. <https://doi.org/10.1016/j.dynatmoce.2008.09.004>
- Watanabe, M., & Nitta, T. (1999). Decadal changes in the atmospheric circulation and associated surface climate variations in the Northern Hemisphere winter. *Journal of Climate*, 12(2), 494–510. [https://doi.org/10.1175/1520-0442\(1999\)012%3C0494:DCITAC%3E2.0.CO;2](https://doi.org/10.1175/1520-0442(1999)012%3C0494:DCITAC%3E2.0.CO;2)
- Webster, P. J., & Yang, S. (1992). Monsoon and ENSO: Selectively interactive systems. *Quarterly Journal of the Royal Meteorological Society*, 118(507), 877–926. <https://doi.org/10.1002/qj.49711850705>
- Wei, K., Mii, H., & Huang, C. Y. (2005). Age model and oxygen isotope stratigraphy of site ODP 1202 in the southern Okinawa Trough, Northwestern Pacific. *Terrestrial, Atmospheric and Oceanic Sciences*, 16, 001–017. [https://doi.org/10.3319/TAO.2005.16.1.1\(OT\)](https://doi.org/10.3319/TAO.2005.16.1.1(OT))
- Wu, B., & Wang, J. (2002). Winter Arctic oscillation, Siberian high and east Asian winter monsoon. *Geophysical Research Letters*, 29(19), 1897. <https://doi.org/10.1029/2002GL015373>
- Wu, W., Tan, W., Zhou, L., Yang, H., & Xu, Y. (2012). Sea surface temperature variability in southern Okinawa Trough during last 2700 years. *Geophysical Research Letters*, 39, L14705. <https://doi.org/10.1029/2012GL052749>
- Wu, R., Chen, W., Wang, G., & Hu, K. (2014). Relative contribution of ENSO and East Asian winter monsoon to the South China Sea SST anomalies during ENSO decaying years. *Journal of Geophysical Research: Atmospheres*, 119, 5046–5064. <https://doi.org/10.1002/2013JD021095>
- Xiang, R., Li, T., Yang, Z., Li, A., Jiang, F., Yan, J., & Cao, Q. (2003). Geological records of marine environmental changes in the southern Okinawa Trough. *Chinese Science Bulletin*, 48(2), 194–199. <https://doi.org/10.1360/03tb9040>
- Xiang, R., Yang, Z., Saito, Y., Guo, Z., Fan, D., Li, Y., ... Chen, M. (2006). East Asia Winter Monsoon changes inferred from environmentally sensitive grain-size component records during the last 2300 years in mud area southwest off Cheju Island, ECS. *Science China Earth Sciences*, 49, 604–614. <https://doi.org/10.1007/s11430-006-0604-1>
- Xiang, R., Sun, Y., Li, T., Oppo, D., Chen, M., & Zheng, F. (2007). Paleoenvironmental change in the middle Okinawa Trough since the last deglaciation: Evidence from the sedimentation rate and planktonic foraminiferal record. *Palaeoogeography Palaoclimatology Palaecology*, 243, 378–393. <https://doi.org/10.1016/j.palaeo.2006.08.016>
- Xiao, S., Li, A., Jiang, F., Li, T., Huang, P., & Xu, Z. (2005). Recent 2000-year geological records of mud in the inner shelf of the East China Sea and their climatic implications. *Chinese Science Bulletin*, 50, 466–471. <https://doi.org/10.1007/BF02897464>
- Xiao, S., Li, A., Liu, J. P., Chen, M., Xie, Q., Jiang, F., ... Chen, Z. (2006). Coherence between solar activity and the East Asian winter monsoon variability in the past 8000 years from Yangtze River-derived mud in the East China Sea. *Palaeoogeography Palaoclimatology Palaecology*, 237, 293–304. <https://doi.org/10.1016/j.palaeo.2005.12.003>
- Xie, S., Hafner, J., Tanimoto, Y., Liu, W., Tokinaga, H., & Xu, H. (2002). Bathymetric effect on the winter sea surface temperature and climate of the Yellow and East China seas. *Geophysical Research Letters*, 29(24), 2228. <https://doi.org/10.1029/2002GL015884>
- Yan, H., Soon, W., & Wang, Y. (2015). A composite sea surface temperature record of the northern South China Sea for the past 2500 years: A unique look into seasonality and seasonal climate changes during warm and cold periods. *Earth Science Reviews*, 141, 122–135. <https://doi.org/10.1016/j.earscirev.2014.12.003>
- Yang, W., Zhou, X., Xiang, R., Wang, Y., Shao, D., & Sun, L. (2015). Reconstruction of winter monsoon strength by elemental ratio of sediments in the East China Sea. *Journal of Asian Earth Sciences*, 114(3), 467–475. <https://doi.org/10.1016/j.jseas.2015.04.010>
- Yu, H., Liu, Z., Berné, S., Jia, G., Xiong, Y., Dickens, G. R., ... Chen, F. (2009). Variations in temperature and salinity of the surface water above the middle Okinawa trough during the past 37kyr. *Palaeoogeography Palaoclimatology Palaecology*, 281, 154–164. <https://doi.org/10.1016/j.palaeo.2009.08.002>
- Zhang, D. (1980). Winter temperature changes during the last 500 years in South China (in Chinese). *Chinese Science Bulletin*, 6, 497–500.
- Zhang, R., Sumi, A., & Kimoto, M. (1996). Impact of El Niño on the East Asian monsoon: A diagnostic study of the '86/'87 and '91/'92 events. *Journal of the Meteorological Society of Japan*, 74(1), 49–62. [https://doi.org/10.2151/jmsj1965.74.1\\_49](https://doi.org/10.2151/jmsj1965.74.1_49)
- Zhang, P., Cheng, H., Edwards, R. L., Chen, F., Wang, Y., Yang, X., ... Johnson, K. R. (2008). A test of climate, Sun, and culture relationships from an 1810-year Chinese cave record. *Science*, 322, 940–942. <https://doi.org/10.1126/science.1163965>
- Zhao, M., Huang, C., & Wei, K. (2005). A 28000 year  $U_{37}^K$  sea-surface temperature record of ODP Site 1202B, the Southern Okinawa Trough. *TAO*, 16, 45–56.
- Zhao, K., Wang, Y., Edwards, R. L., Chen, H., Liu, D., & Kong, X. (2015). A high-resolved record of the Asian Summer Monsoon from Dongge Cave, China for the past 1200 years. *Quaternary Science Reviews*, 122, 250–257. <https://doi.org/10.1016/j.quascirev.2015.05.030>
- Zheng, X., Li, A., Wan, S., Jiang, F., Kao, S. J., & Johnson, C. (2014). ITCZ and ENSO pacing on East Asian winter monsoon variation during the Holocene: Sedimentological evidence from the Okinawa Trough. *Journal of Geophysical Research: Oceans*, 119, 4410–4429. <https://doi.org/10.1002/2013JC009603>
- Zhou, M., & Wang, H. (2014). Late winter sea ice in the Bering Sea: Predictor for maize and Rice production in Northeast China. *Journal of Applied Meteorology and Climatology*, 53(5), 1183–1192. <https://doi.org/10.1175/JAMC-D-13-0242.1>
- Zhou, X., Yang, W., Xiang, R., Wang, Y., & Sun, L. (2014). Re-examining the potential of using sensitive grain size of coastal muddy sediments as proxy of winter monsoon strength. *Quaternary International*, 333, 173–178. <https://doi.org/10.1016/j.quaint.2013.12.013>